



Published in final edited form as:

Pediatr Blood Cancer. 2017 June ; 64(6): . doi:10.1002/pbc.26350.

Desmoplastic infantile astrocytoma/ganglioglioma with rare *BRAF* V600D mutation

Ashley Greer¹, Nicholas K. Foreman², Andrew Donson², Kurtis D. Davies¹, and B. K. Kleinschmidt-DeMasters^{1,3,4}

¹Department of Pathology, The University of Colorado School of Medicine, Aurora, Colorado

²Department of Pediatrics, Children's Hospital Colorado, Aurora, CO

³Department of Neurosurgery, The University of Colorado School of Medicine, Aurora, Colorado

⁴Department of Neurology, The University of Colorado School of Medicine, Aurora, Colorado

Abstract

Background—Desmoplastic infantile astrocytoma (DIA) and desmoplastic infantile gangliogliomas (DIGs) are rare, massive, cystic and solid tumors of infants usually found in superficial cerebral hemispheres. They manifest prominent desmoplastic stroma, admixed neoplastic astrocytes, primitive-appearing small cells, and additional neoplastic ganglion cells in the case of DIGs. While v-Raf murine sarcoma viral oncogene homolog B (*BRAF*) mutation is found in up to 50% of pediatric gangliogliomas, two recent studies found that it was rare in DIA/DIGs; we sought to assess *BRAF* status in DIA/DIGs from our institution.

Procedure—Departmental files from 2000 to 2016 were reviewed to identify cases. Clinical, neuroimaging, histological, and immunohistochemistry (IHC) features were assessed; the latter included IHC for astrocytic and neuronal markers and BRAF VE1. *BRAF* mutational assessment by Sanger and next-generation sequencing was attempted in all cases.

Results—All six identified cases (four males—two females; three DIA—three DIG) occurred in children <1-year old, were large, cerebral-hemispheric, cystic and solid, and enhancing tumors. Only one case, a DIG with prominent aggregates of neoplastic ganglion cells, showed either BRAF VE1 IHC positivity or mutation by Sanger and next-generation sequencing (rare c. 1799_1800delinsAT; p. V600D). Four of six archival cases were BRAF VE1 IHC negative, but failed mutational sequencing.

Conclusion—Five of six classic DIA/DIGs were negative for *BRAF* mutation; previous series have identified *BRAF* mutation in two of 18 and one of 14 cases, although all were the more common *BRAF*V600E. We were unable to find other examples of glial tumors in public databases

Correspondence: B. K. Kleinschmidt-DeMasters, Department of Pathology, University of Colorado School of Medicine, 12605 E. 16th Avenue, F 768, Aurora, CO 80045. bk.demasters@ucdenver.edu.

Presented in abstract format at the College of American Pathologists annual meeting, CAP' 16, September 25–28, 2016, Las Vegas, Nevada.

CONFLICT OF INTEREST

The authors declare that there is no conflict of interest.

with this rare *BRAF*V600D mutation. Identification of BRAF mutational opens the possibility of BRAF-targeted therapies for the subset of DIA/DIG that clinically progress postresection.

Keywords

astrocytoma; BRAF; desmoplastic; ganglioglioma; infant

1 | INTRODUCTION

Desmoplastic infantile astrocytoma (DIA) and desmoplastic infantile ganglioglioma (DIG) are massive, enhancing, cystic and solid, superficially located tumors usually found in the cerebral hemisphere. The majority occur in infants less than 24 months of age, with a median of 6 months.¹ Tumors are slow growing, and World Health Organization (WHO) grade I, despite their ominous neuroimaging appearance, and thus are usually curable by gross total surgical excision.¹ However, recent literature reviews^{2,3} emphasize that in the subset in which gross total resection is not feasible due to deep location, massive size, and/or bilateral extension,³ further surgical, radiation therapy, or chemotherapy has been necessary. Thus, identifying mutations for which targeted therapies exist has clinical value in treating a subset of these tumors.

DIA and DIG were originally described as separate tumor entities,^{4,5} but given their similar clinical, neuroimaging, and pathological features, these have been categorized together in the WHO classification since the 2000 edition.^{1,5,6} Unifying features of DIA/DIG were recently further emphasized by Gessi et al., who, by genome-wide DNA copy number analysis, showed that large chromosomal changes were rare in either tumor type, but both shared focal genomic losses in 5q13,3, 21q22,11, and 10q21.3.⁷ They concluded that DIA and DIG “represent a histological spectrum of the same tumor rather than two separate entities.”⁷

DIA/DIG is characterized by frequent, but not invariable, dural attachment and a reticulin-rich, spindle cell stroma containing connective tissue due to the prominent leptomeningeal involvement.¹ The potential for histological misdiagnosis exists due to the fact that these tumors contain varying proportions of neoplastic glial, neuronal, and poorly differentiated cells, the latter lending a “small blue cell tumor” feature to the tumor. The primitive-appearing element can lead to mis-diagnosis of a WHO grade IV embryonal tumor. DIA contains only the primitive element plus astrocytic tumor cells, while in DIG, the astrocytic tumor population predominates but, in addition, a neoplastic ganglion cell component is identified. The latter is usually composed of larger sized ganglion cells.

While the presence of ganglion cells in DIG could suggest some biological overlap with conventional ganglioglioma, the latter lacks the very young patient age, massive size, and rich desmoplastic investiture of DIG. Gangliogliomas in pediatric patients are known to harbor v-Raf murine sarcoma viral oncogene homolog B (*BRAF*) V600E mutations, variably reported as 35%,⁸ 50%,⁹ and >60%¹⁰ of cases. This has prompted several previous studies looking for BRAF mutations in DIAs and DIGs.^{7,11–13} By varying methodologies, *BRAF*V600E mutation was found in one of two cases (listed as DIG),¹³ one of 14 cases (listed as DIA),⁷ and two of 18 cases (listed as one DIA and one DIG).¹¹ In addition, single

cases with *BRAF*V600E mutation (listed as DIA)¹² and a *BRAF* fusion (listed as DIG) (*FXR1-BRAF*, where *FXR1* is fragile X mental retardation syndrome-related protein 1)¹⁴ have been reported.

These previous findings prompted us to assess all newly diagnosed DIAs and DIGs for *BRAF* mutation. This recently resulted in the discovery of a ganglion cell rich DIG with a rare, previously unreported *BRAF*V600D mutation (amino acid substitution at position 600 in *BRAF*, from a valine [V] to an aspartic acid [D]) rather than the far more common *BRAF* V600E (amino acid substitution at position 600 in *BRAF*, from a valine [V] to a glutamic acid [E]) alteration.

We report this case to emphasize that mutational analysis, rather than *BRAF* VE1 immunohistochemistry (IHC), which only identifies the mutant protein resulting from the far more common V600E mutation, may be required to fully identify *BRAF*-mutated examples. We also tested retrospectively five additional cases in our files to add to the numbers of tested cases in the literature.

2 | MATERIALS AND METHODS

2.1 | Patient accrual

All studies were conducted in compliance with local and federal research protection guidelines and institutional review board regulations (COMIRB #95-500 and 05-149). Retrospective review of the neurooncology database at Children's Hospital Colorado was conducted to identify patients who were diagnosed at our institution with DIAs and DIGs. Eligible patients had been initially seen, received neurosurgical resection of tumor, or been seen in clinical follow-up between, with closure date of study in January 2016. Clinical outcome was obtained from the neurooncology database, supplemented by the medical records. Clinical progression was determined by the neurooncologist on the study, which was also responsible for patient follow-up and care, and included evaluation of neuroimaging features. Extent of resection was determined by postoperative neuroimaging.

2.2 | Routine histology and IHC

Tissues were fixed in 10% buffered formalin, paraffin-embedded, and cut at 5 μ m. All cases were stained with Harris hematoxylin and eosin and Gomori reticulin. IHC was performed on formalin-fixed, paraffin-embedded tumor tissue sections. IHCs included glial fibrillary acidic protein (GFAP; Dako Corporation, Carpinteria, CA; polyclonal, 1:2,500, no antigen retrieval), MIB-1 (Dako Corporation; monoclonal, 1:50 dilution, antigen retrieval), synaptophysin (Biogenex; catalog number Am363; clone Snp88), NeuN (Millipore; catalog number MAB377), antineurofilament (Cell Marque; clone 2F11), and/or chromogranin (Ventana; catalog number 760–2519).

For *BRAF* VE1, antigen retrieval was performed using heat-induced epitope retrieval high pH Ventana Cell Conditioning Solution (Ventana, Tucson, AZ) for 60 min at 95–100°C. Incubation with primary antibody at a 1:100 dilution (mouse monoclonal anti-human *BRAF*^{V600E} clone VE1, Cat#E1929; Spring Bioscience, Pleasanton, CA) was performed at

42°C for 48 min. Sections were then stained with the Ventana IHC Multimer alkaline phosphatase staining kit. All sections were counter-stained with hematoxylin.

2.3 | *BRAF* gene mutation sequencing

Direct (Sanger) sequencing was performed as previously described.⁹ Library preparation for next-generation sequencing was performed using the Illumina TruSight Tumor 26 kit as per the manufacturer's instructions (with minor modifications). This kit amplifies selected regions of 26 cancer-related genes. Libraries were sequenced on the Illumina MiSeq platform for a targeted depth of no less than 500,× for any individual amplicon. A custom-built bioinformatics pipeline utilizing GSNAP for sequence alignment and FreeBayes for variant calling was employed for data analysis. All genomic regions were verified to be covered by at least 500 sequencing reads and identified variants were manually inspected using Integrative Genomics Viewer (Broad Institute).

3 | RESULTS

Six patients were identified (four males–two females), ranging in age from 1 to 12 months of age (see Table 1). There were three DIAs and three DIGs, including one with prominent aggregates of large ganglion cells (Patient 6). All patients were within the classic, very young age range for DIA/DIG.

Magnetic resonance imaging (MRI) features were consistent with DIA/DIG in all cases, providing pathological–neuroimaging correlation. There were overlapping MRI features regardless of DIA or DIG status (Fig. 1). All tumors were cerebral hemispheric in location, large, cystic, and enhancing. Patients 1 (Fig. 1A) and 6 (Fig. 1D) had multicystic tumors, Patients 2 (Fig. 1B) and 4 (Fig. 1C) had tumors with particularly large enhancing nodules, and Patients 3 (Fig. 1E) and 5 (Fig. 1F) showed unilocular lesions with more obvious superficial, dural-based relationship. Of the six patients, four underwent a complete resection, one had a near-total resection, and the last patient had a subtotal resection; this is detailed in Table 1.

All tumors contained a connective tissue rich component that predominated in the superficial portions of the tumor and showed numerous interspersed cytologically bland astrocytic tumor cells (Fig. 2A). These areas manifested a reticulin-rich matrix (Fig. 2B). Tumor cells in all six examples were mostly astrocytic, as proven by IHC for GFAP (Fig. 2C). DIAs contained little or no ganglion cell component and no synaptophysin immunoreactivity (Fig. 2D). A small cell component was identified in all examples, the latter often with increased cell cycle labeling. DIGs additionally contained variable numbers of larger sized ganglion cells with immunoreactivity for neuronal markers. In Patient 6, classic DIA areas were identified in the tumor identical to those seen in DIAs, as expected (Figs. 3A and 3B). In addition, discrete aggregates containing numerous large, closely juxtaposed, tumor ganglion cells were also found (Fig. 3C). Ganglion tumor cells manifested abundant basophilic cytoplasm, large vesicular nuclei, nucleoli, Nissl substance (Fig. 3C), and strong cytoplasmic synaptophysin immunoreactivity, which further highlighted their bizarre shapes (Fig. 3D). Unlike pleomorphic xanthoastrocytoma or ordinary ganglioglioma, no perivascular nonneoplastic lymphocytic cuffing, eosinophilic granular bodies, or Rosenthal

fibers were present. As is typical of some DIA/DIG, occasional areas showed extension of tumor along Virchow–Robin spaces.

BRAF VE1 IHC was negative for Patients 1–5 and was equivocal for Patient 6. That was the sole example found to have a *BRAF* mutation, which was detected using both Sanger and next-generation sequencing. This proved to be a *BRAFV600D* mutation (amino acid substitution at position 600 in *BRAF*, from a valine [V] to an aspartic acid [D]) rather than the far more common *BRAFV600E* (amino acid substitution at position 600 in *BRAF*, from a valine [V] to a glutamic acid [E]) alteration. A second case (Patient 4) was negative for *BRAF* mutation, which was detected using next-generation sequencing. The remaining four archival cases failed both Sanger and next-generation sequencing, but were definitely negative on BRAF VE1 IHC.

Although the clinical outcome was favorable in all six of our patients and all remained alive 9–195 months post diagnosis (see Table 1), other authors have described examples of DIA/DIG with progressive disease.² In our cohort, one child developed progressive leptomeningeal spread, a known but uncommon complication of DIA/DIG², but responded to chemotherapy. Another child required chemotherapy at the time of diagnosis, again without recurrence following the treatment. Neither of these two patients (Patients 3 and 2) had *BRAF* mutation. Thus, neither, in retrospect, could have benefited from *BRAF*-targeted therapy.

4 | DISCUSSION

DIA/DIGs are rare tumors overall, constituting just 22 of over 6500 central nervous system tumors from patients of all ages in the University of Virginia archive of consultation cases, as reported by VandenBerg.⁴ However, in infants, up to 15.8% of brain tumors are DIA/DIG.¹ Thus, better understanding of the biological features of these tumors is important, although rarity precludes any single institution's ability to accrue large numbers of cases, explaining the relatively modest size of our patient cohort (n=6) in this study from a single institution. Only the single-institution series of 16 patients of Jurkiewicz et al.¹⁵ is larger, while the above-cited studies of 14⁷ and 18¹¹ patients drew their cohorts from more than one institution.

Our study not only expands the numbers of DIA/DIGs tested for *BRAF* mutation, but additionally documents a unique *BRAFV600D* mutation. We report this case due to our inability to locate any *BRAFV600D* mutations in gliomas of any type in the Catalogue of Somatic Mutations in Cancer (<http://www.sanger.ac.uk/cosmic>) or cBioPortal for Cancer Genomics (<http://cbioportal.org>) databases. Although our case with a *BRAF* mutation was a DIG with significant numbers of neoplastic ganglion cells, two of our other DIGs were negative. This correlates with previously reported examples in that *BRAFV600E* mutation has variably been histologically classified as either DIA or DIG (see above). Thus, there does not appear to be correlation between *BRAF* mutational status and the presence or absence of ganglion cells in these tumors. This may parenthetically reinforce the notion that these tumors are not different entities since DIA or DIG may, or may not, show *BRAF* mutation.

We suggest that assessing *BRAF* mutational status beyond simply BRAF VE1 IHC may be necessary to truly understand the percentage of DIAs/DIGs with *BRAF* mutation. Whether tumors with uncommon (noncanonical) BRAF mutations such as V600D are still amenable to targeted therapies for BRAF V600E, such as vemurafenib or dabrafenib, is unknown. Targeted therapies for *BRAF*V600E mutated tumors are unknown. Although the clinical outcome was favorable in all six of our patients (see Table 1), other authors have described examples of DIA/DIG with progressive disease² that could potentially respond to targeted therapy if a *BRAF* mutation is demonstrated.

Interestingly, while we were unable to identify *BRAF*V600D mutations in gliomas of any type, including DIA/DIG in standard databases, this mutation is not unheard of in systemic malignancies. For example, in systemic melanomas, while the majority of cases with BRAF mutations manifest the common *BRAF*V600E (seen in 90%), *BRAF*V600K mutation is found in 5–6% and *BRAF*V600D is identified infrequently; some data suggest that melanomas with these rare mutations types might respond to BRAF inhibitors.¹⁶ Thus, identifying any type of *BRAF* mutation in a DIA/DIG opens the possibility of use of targeted therapies, if needed for subtotally resected cases with recurrence, or even rare leptomeningeal dissemination.²

Acknowledgments

Grant sponsor: Olivia Caldwell Foundation; Grant sponsor: Morgan Adams Foundation; Grant sponsor: Molecular Pathology Shared Resource of the University of Colorado's NIH/NCI Cancer Center; Grant number: P30CA046934.

The authors thank Mrs. Diane Hutchinson for manuscript preparation, Ms. Lisa Litzenberger for photographic expertise, Dr. Patrick Mann for molecular database searching, and Dr. Dara Aisner for helpful comments.

Abbreviations

BRAF	v-Raf murine sarcoma viral oncogene homolog B
DIA	desmoplastic infantile astrocytoma
DIG	desmoplastic infantile ganglioglioma
GFAP	glial fibrillary acidic protein
IHC	immunohistochemistry
WHO	World Health Organization

References

1. Brat, D., VandenBerg, S., Figarella-Branger, D., Reuss, D. Desmoplastic infantile astrocytoma and ganglioglioma. In: Louis, DN, Ohgaki, H, Wiestler, OD., et al., editors. WHO Classification of Tumours of the Central Nervous System. Lyon: IARC; 2016. p. 144-146.
2. Hummel TR, Miles L, Mangano FT, Jones BV, Geller JI. Clinical heterogeneity of desmoplastic infantile ganglioglioma: A case series and literature review. *J Pediatr Hematol Oncol.* 2012; 34(6):e232–e236. [PubMed: 22735886]

3. Gelabert-Gonzalez M, Serramito-Garcia R, Arcos-Algaba A. Desmoplastic infantile and non-infantile ganglioglioma. Review of the literature. *Neurosurg Rev.* 2010; 34(2):151–158. [PubMed: 21246390]
4. VandenBerg SR. Desmoplastic infantile ganglioglioma and desmoplastic cerebral astrocytoma of infancy. *Brain Pathol.* 1993; 3(3):275–281. [PubMed: 8293187]
5. Taratuto, AL., VandenBerg, SR., Rorke, LB. Desmoplastic infantile astrocytoma and ganglioglioma. In: Kleihues, P., Cavenee, WK., editors. *WHO Classification of Tumors, Pathology and Genetics: Tumors of the Nervous System.* Lyon: IARC; 2000. p. 99-102.
6. Brat, D., VandenBerg, S., Figarella-Branger, D., Taratuto, A. Desmoplastic infantile astrocytoma and ganglioglioma. In: Louis, D., Ohgaki, H., Wiestler, O., Cavenee, W., editors. *WHO Classification of Tumours of the Central Nervous System.* Lyon: IARC; 2007. p. 96-98.
7. Gessi M, Zur Muhlen A, Hammes J, Waha A, Denkhaus D, Pietsch T. Genome-wide DNA copy number analysis of desmoplastic infantile astrocytomas and desmoplastic infantile gangliogliomas. *J Neuropathol Exp Neurol.* 2013; 72(9):807–815. [PubMed: 23965740]
8. Qaddoumi I, Orisme W, Wen J, et al. Genetic alterations in uncommon low-grade neuroepithelial tumors: BRAF, FGFR1, and MYB mutations occur at high frequency and align with morphology. *Acta Neuropathol.* 2016; 131(6):833–845. [PubMed: 26810070]
9. Donson AM, Kleinschmidt-DeMasters BK, Aisner DL, et al. Pediatric brainstem gangliogliomas show BRAF(V600E) mutation in a high percentage of cases. *Brain Pathol.* 2014; 24(2):173–183. [PubMed: 24238153]
10. Berghthold G, Bandopadhyay P, Hoshida Y, et al. Expression profiles of 151 pediatric low-grade gliomas reveal molecular differences associated with location and histological subtype. *Neuro Oncol.* 2015; 17(11):1486–1496. [PubMed: 25825052]
11. Koelsche C, Sahm F, Paulus W, et al. BRAF V600E expression and distribution in desmoplastic infantile astrocytoma/ganglioglioma. *Neuropathol Appl Neurobiol.* 2014; 40(3):337–344. [PubMed: 23822828]
12. Karabagli P, Karabagli H, Kose D, Kocak N, Etus V, Koksal Y. Desmoplastic non-infantile astrocytic tumor with BRAF V600E mutation. *Brain Tumor Pathol.* 2014; 31(4):282–288. [PubMed: 24531831]
13. Dougherty MJ, Santi M, Brose MS, et al. Activating mutations in BRAF characterize a spectrum of pediatric low-grade gliomas. *Neuro Oncol.* 2010; 12(7):621–630. [PubMed: 20156809]
14. Zhang J, Wu G, Miller CP, et al. Whole-genome sequencing identifies genetic alterations in pediatric low-grade gliomas. *Nat Genet.* 2013; 45(6):602–612. [PubMed: 23583981]
15. Jurkiewicz E, Grajkowska W, Nowak K, Kowalczyk P, Walecka A, Dembowska-Baginska B. MR imaging, apparent diffusion coefficient and histopathological features of desmoplastic infantile tumors—own experience and review of the literature. *Childs Nerv Syst.* 2015; 31(2):251–259. [PubMed: 25416471]
16. Ascierto PA, Kirkwood JM, Grob JJ, et al. The role of BRAF V600 mutation in melanoma. *J Transl Med.* 2012; 10:85. [PubMed: 22554099]

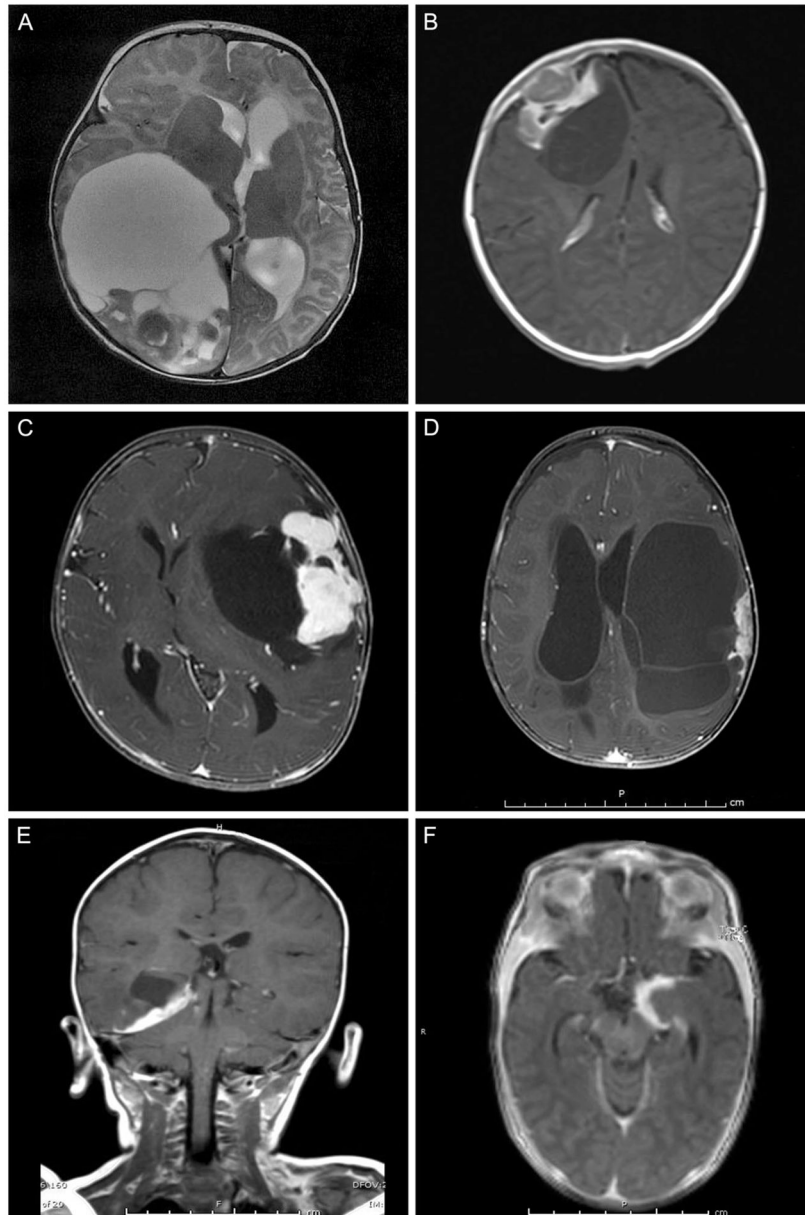


FIGURE 1.

All six tumors showed classic neuroimaging features of DIA/DIG, providing pathological-neuroimaging correlation in that all were cerebral hemispheric in location, large, cystic, and enhancing. Patients 1 (A) and 6 (D) had multicystic tumors, Patients 2 (B) and 4 (C) had tumors with particularly large enhancing nodules, and Patients 3 (E) and 5 (F) showed unilocular lesions with more obvious superficial, dural-based relationship. Axial magnetic resonance imaging, A–D and F; coronal, E; T2-weighted MRI, A; T1-weighted MRI with gadolinium, B–F

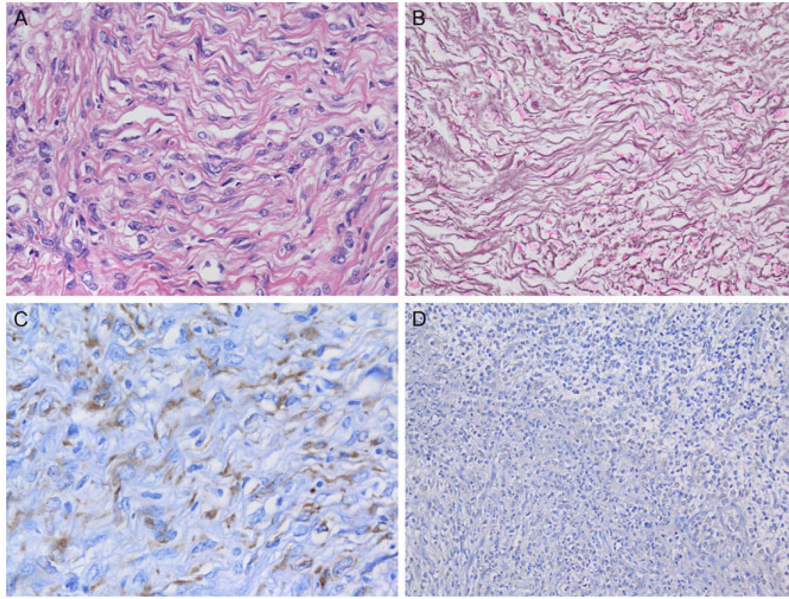


FIGURE 2.

All tumors contained a connective tissue-rich component that predominated in the superficial portions of the tumor and showed numerous interspersed cytologically bland astrocytic tumor cells (A). These areas manifested a reticulin-rich matrix (B). Tumor cells in all six examples were mostly astrocytic, as proven by IHC for glial fibrillary acidic protein (GFAP) (C). DIAs contained little or no ganglion cell component and no synaptophysin immunoreactivity (D). Patient 1 illustration: (A) Hematoxylin and eosin, 400×; (B) Gomori reticulin stain, 400×; (C) GFAP IHC with hematoxylin counterstain, 400×; (D) synaptophysin IHC with hematoxylin counterstain, 200×

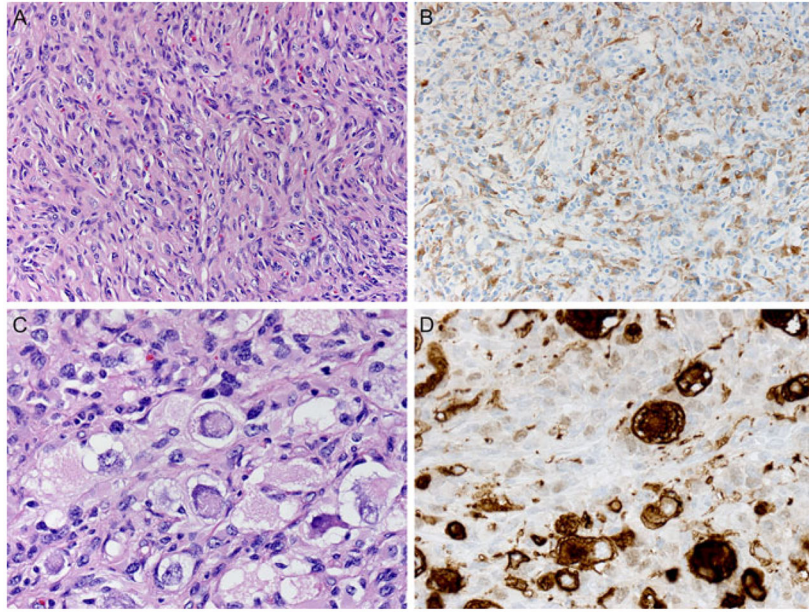


FIGURE 3.

In DIGs, areas were identified in the tumors identical to those seen in DIAs, as expected (A and B). In addition, discrete aggregates containing numerous large, closely juxtaposed tumor ganglion cells were also found and were most conspicuous in Patient 6 where they occurred as large aggregates (C). Ganglion tumor cells manifested abundant basophilic cytoplasm, large vesicular nuclei, nucleoli, and Nissl substance (C) and strong cytoplasmic synaptophysin immunoreactivity, which further highlighted their bizarre shapes (D). (A) Hematoxylin and eosin, 400×; (B) GFAP immunohistochemistry with hematoxylin counterstain, 400×; (C) hematoxylin and eosin, 600×; (D) synaptophysin immunohistochemistry with hematoxylin counter-stain, 600×

TABLE 1

Desmoplastic infantile astrocytoma/ganglioglioma cases

Patient, age, gender	Location, diagnosis, extent of resection	BRAF VE1	BRAF mutation	Clinical follow-up, length of survival (in months)
1, 3 months, F	R parietooccipital region DIA NTR	NEG	Failed Sanger, next-generation sequencing, qPCR mutational analyses	Alive with no recurrence 9 months
2, 1 month, M	R frontal lobe DIA STR	NEG	Failed Sanger, next-generation sequencing, qPCR mutational analyses	Treated at time of diagnosis with carboplatin/etoposide Alive with no recurrence 93 months
3, 11 months, F	R parietooccipital region DIA CR	NEG	Failed Sanger, next-generation sequencing, qPCR mutational analyses	Progressive leptomeningeal spread noted 2 months postoperatively. Therapy with high-dose chemotherapy, then temozolomide. Alive with no additional recurrence 195 months
4, 7 months, M	L cerebral hemisphere DIG CR	NEG	Mutation not identified on next-generation sequencing	Alive with no recurrence 8 months
5, 3 months, M	L temporal lobe DIG CR	NEG	Failed Sanger, next-generation sequencing, qPCR mutational analyses	Alive with no recurrence 36 months
6, 1 year, M	L cerebral hemisphere DIG CR	Equivocal Immunostaining	Mutation present (c.1799_1800TG>AT;V600D)	Alive with no recurrence 9 months

CR, complete resection; DIA, desmoplastic infantile astrocytoma; DIG, desmoplastic infantile ganglioglioma; F, female; L, left; M, male; NEG, negative; NTR, near total resection; POS, positive for mutation; qPCR, quantitative PCR. R, right; STR, subtotal resection;